



CrossMark
click for updates

Cite this: *RSC Adv.*, 2015, 5, 71203

Rapid prototyping of microchannels with surface patterns for fabrication of polymer fibers†

Payton J. Goodrich,^a Farrokh Sharifi^a and Nastaran Hashemi^{*ab}

Microfluidic technology has provided innovative solutions to numerous problems, but the cost of designing and fabricating microfluidic channels is impeding its expansion. In this work, Shrinky-Dink thermoplastic sheets are used to create multilayered complex templates for microfluidic channels. We used inkjet and laserjet printers to raise a predetermined microchannel geometry by depositing several layers of ink for each feature consecutively. We achieved feature heights over 100 μm , which were measured and compared with surface profilometry. Templates closest to the target geometry were then used to create microfluidic devices from soft-lithography with the molds as a template. These microfluidic devices were in turn used to fabricate polymer microfibers using the microfluidic focusing approach to demonstrate the potential that this process has for microfluidic applications. Finally, an economic analysis was conducted to compare the price of common microfluidic template manufacturing methods. We showed that multilayer microchannels can be created significantly quicker and cheaper than current methods for design prototyping and point-of-care applications in the biomedical area.

Received 30th July 2015
Accepted 14th August 2015

DOI: 10.1039/c5ra15154f

www.rsc.org/advances

Introduction

Microfluidics is a rapidly growing field of research that is creating innovative solutions to environmental monitoring,^{1–3} biological technology,^{4,5} and energy production.^{6–8} Recently, researchers have been exploring the possible uses of microfluidics in biomedical diagnostics^{9–15} and biocompatible polymer microfiber fabrication.^{16–24} Microfluidic diagnostic devices show a lot of promise as they have high portability, reduced analysis time, and inexpensive production compared to benchtop instruments. Beyond this, researchers have already shown their ability to detect influenza,¹⁰ HIV,¹¹ tumors,^{12,13} and other ailments with microfluidic diagnostic techniques. Polymer microfibers can be made by a microfluidic focusing approach, which allows control over the shape and size of the fibers.^{18,19} These fibers show promise as substrates for drug delivery,^{16,19} cell growth,^{17,19,22} and tissue engineering.^{19,20} The high cost and slow production of the popular silicon wafer template for creating microchannels, however, is limiting the expansion of this field. Silicon wafers are chemically inert and provide highly accurate features due to their high purity crystalline structure, but they require a large amount of time and resources to manufacture.²⁵ Lower production costs of microfluidic devices

are highly desirable for their point of care diagnostics in resource poor environments.⁹

In recent years, thermoplastics have been gaining momentum as a substrate for imprinting microscale grooves with a single height to create microfluidic channels.^{26–28} A two-dimensional microchannel geometry is printed onto the thermoplastic sheet, which when heated, shrinks in the horizontal plane and grows vertically. These molds are then used as a rigid template for soft-lithography using polydimethylsiloxane (PDMS) or other polymers.²⁹ The liquid polymer is poured onto the template and then solidifies, creating a negative image of the template. Shrinky-Dink Shrinkable Plastics in particular have become a common choice of thermoplastic sheets among researchers, due to their desirable qualities and ability to create simple two-dimensional patterns affordably with laserjet printers.³⁰ The drawbacks of this method are that there is a limited feature depth and material incompatibilities.^{30,31} To our knowledge, no researchers have successfully reported quantitatively or qualitatively microfluidic multilayer channels with three dimensional features from thermoplastics, although Grimes *et al.* suggests to the possibility.³⁰

Multilayer features from laserjet printing has been achieved in previous work using copper as a printing substrate.³² Copper as a substrate has proven as a legitimate method for prototyping, but requires more expensive materials and complicated processes. Copper substrates require special means for printing, such as copper coated films, copper etchant CE-100, dicing tape, acetone, and special registration black toner.

^aDepartment of Mechanical Engineering, Iowa State University, Ames, IA 50011, USA.
E-mail: nastaran@iastate.edu

^bAmes National Laboratory, Ames, IA 50011, USA

† Electronic supplementary information (ESI) available. See DOI: 10.1039/c5ra15154f

Although viable, copper substrates are less readily available for implementation.

3D printers have been investigated as a means to print microfluidic channels affordably.^{33,34} These methods have some practical uses, but are ultimately restricted to low resolution products. For example, the MiiCraft+ ® printer has a lateral resolution of approximately 56 µm and a vertical resolution of 30 µm, meaning that the microchannel dimensions are limited to multiples of these numbers. Furthermore, 3D printed channels have been found to have greatly distorted side-wall roughness.³⁴ Until 3D printer technology improves, it has a limited range of use in microfluidic applications.

Poly(methyl methacrylate) (PMMA) has also been reported as a substrate for soft-lithography.^{11,35} By using highly accurate CNC micromills and precise toolbits, a PMMA workpiece can have a positive relief microchannel cut into its surface. This process can result in higher resolution than a 3D printer, but it still has an expensive overhead cost.

Microfibers can be fabricated by either microfluidic focusing or industrial spinning techniques.¹⁹ Each of these methods has their own unique advantages and limitations: while industrial spinning techniques and high-speed extrusion are capable of rapidly creating large quantities of fibers, microfluidic focusing is far more suitable for applications involving biological matter such as cell growth, drug delivery, and tissue engineering. This is because spinning techniques require extreme reaction conditions such as high shear, high melt temperatures, high voltage, and rapid cooling. Microfluidic focusing, on the other hand, caters to very mild reaction conditions. This approach is also flexible across various geometries and materials.^{19,20} Various shapes of fibers have been reported^{16,19,20} with fiber diameters ranging from nanometer scale to several hundred microns.²⁰ Finally, a single microfluidic channel is capable of creating an assortment of unique fibers by adjusting the flow rates, whereas industrial

spinning techniques would require some form of retooling to change the fiber's characteristics.²⁰

The method proposed in this paper can be used to rapidly create microfluidic mold templates with variable height features that may serve as stand-alone templates or as prototypes for future silicon wafer template generation. In other words, the functionality of microfluidic devices fabricated using the process outlined in this paper is not limited to creating microfibers. Rather, many types of microfluidic applications are theoretically possible with microfluidic devices made from this method for creating templates, which could benefit a large spectrum of research with lab on a chip applications.

In this work, we successfully create multilayer microfluidic templates using Shrinky-Dink thermoplastic sheets as a printing substrate. The microchannel has chevron grooves on both bottom and top sides of the channel previously reported in literature.^{16,36} The capability of the mold template was then demonstrated by using it as a template to create a microfluidic device from PDMS, which was in turn used to create polycaprolactone (PCL) microfibers similar to ones made with a silicon wafer template.¹⁶ PCL microfibers have many applications in the medical field. These microfibers are biocompatible and can be used for biomedical applications such as regenerative medicine and tissue engineering.

Materials and methods

In choosing the methodology and equipment used for rapid prototyping, low cost materials were chosen for accessibility to future microchannel prototyping. A HP F2400 All-In-One Inkjet printer was used to print consecutive layers of two-dimensional geometries onto Shrinky-Dink Ink Jet Shrinkable Plastic with HP 60 black ink. "Black ink only" processes were chosen for consistent ink properties.

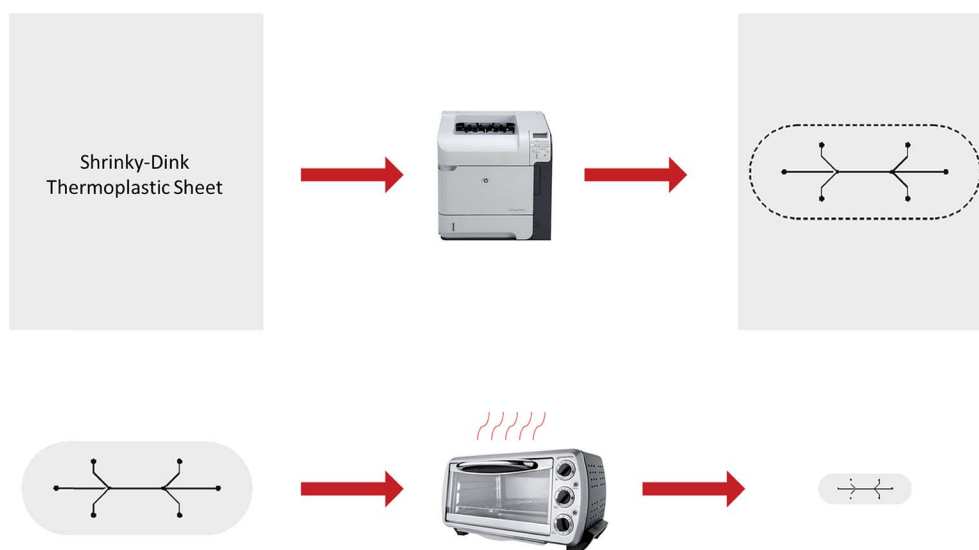


Fig. 1 Process for fabricating a microfluidic template. Ink is deposited onto a thermoplastic sheet which is cut out and heated in an oven to shrink to one third of its original size.

In a second set of trials, an HP LaserJet P4015dn printer was used to print consecutive layers of two-dimensional geometries onto Shrinky-Dink "Crystal Clear" Shrinkable Plastic with HP 64X High Yield Black Original LaserJet Toner. The two different methods allow for the cross comparison of inkjet printing, which uses a liquid ink, *versus* laserjet printing, which uses a powder ink.

SolidWorks was used to design microchannel geometries. Although SolidWorks allows the option of printing to scale, most types of printers will distort this value internally. Instead, an iterative process was developed where the print size was scaled, the geometries were printed onto the Shrinky-Dink plastic, the plastic was uniformly heated, and the resulting features were measured and compared to the desired final feature size. The scaling factor was adjusted in a series of trials to finally find that a scaling factor of 246% would produce the desired two-dimensional feature sizes after baking. Both the inkjet and laserjet printers yielded the same scaling factor, indicating this value may be the most accurate across other printers as well.

To create multilayer geometries, two or more two-dimensional geometries are printed onto the same sheet of Shrinky-Dink plastic. The heights of the two-dimensional geometries are dictated by the number of times the geometry is printed onto the thermoplastic sheet; printing the same two-dimensional geometry several times increases the deposition of ink toner onto the Shrinky-Dink sheet. In this way, features with variable microscale heights are raised similar to the operation of commercial 3D printers. Where 3D printers use plastic to create thickness, however, this method replaces layers of plastic with layers of ink printed consecutively on top of one another, allowing ample time to dry between prints.

A two-dimensional base layer was made by printing several times on the same sheet until a desirable thickness is achieved. Second and third layers can be raised on top of each other by printing a two-dimensional geometry that is constrained by the borders of the layer before it. For our purposes, a microchannel geometry was chosen as the base layer, as seen in our previous work.³⁶ Next, chevron grooves were printed on top of the microchannel with a width of 100 μm spaced 150 μm apart. A schematic for the target geometry can be found in Fig. S1 of the ESI.†

After all layers of the two geometries were printed and dried, the microchannel template was cut from the Shrinky-Dink Shrinkable Plastic. The template was placed on a piece of brown paper and covered loosely with a strip of wax paper. It was then placed in a pre-heated oven at 135 $^{\circ}\text{C}$ for 3–5 minutes until the template was flat. After waiting an additional twenty seconds, the template was removed from the oven and pressed flat by gently sandwiching it between two surfaces to remove any remaining curvature attained in the shrinking process. The overall process for creating microfluidic templates is illustrated in Fig. 1.

In order to quantify the feature height and roughness that can be achieved by consecutive printing, microchannels with one to four layers of inks were prepared and measured by profilometry techniques. These findings are presented in Fig. 2. A

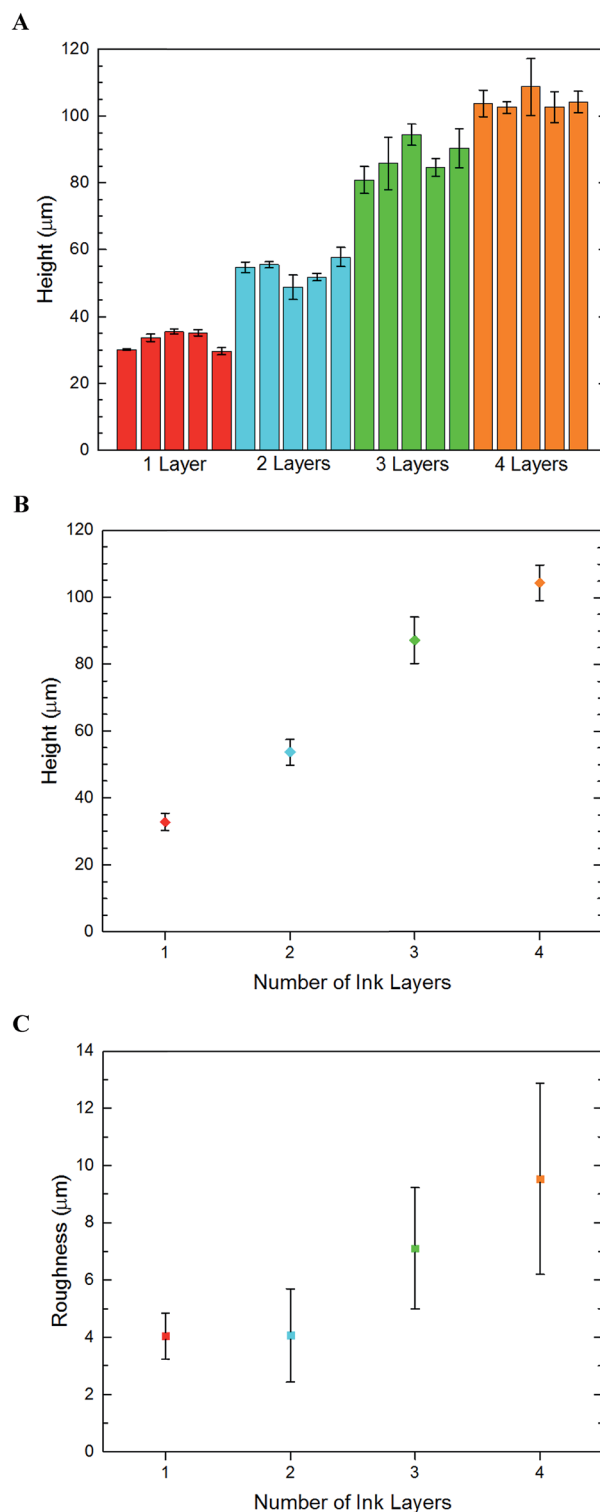


Fig. 2 Profilometry measurements of test channels. Data points are the mean and error bars are the standard deviation of the samples. (A) Individual height results of all channels ($n = 3$). (B) Average height for the combined results of (A). The average heights are 32.38 μm , 53.72 μm , 87.22 μm , and 104.42 μm respectively. The standard deviations are 2.63 μm , 3.86 μm , 6.93 μm , and 5.40 μm respectively. (C) Average roughness for the combined results of (A). The average values are 4.04 μm , 4.06 μm , 7.11 μm , and 9.53 μm respectively. The standard deviations are 0.80 μm , 1.63 μm , 2.12 μm , and 3.34 μm respectively.

guide to how these measurements were made can be found in Fig. S2 of the ESI.†

Results and discussion

The number of print layers per feature was varied and the resulting feature heights were recorded. Channel height, chevron height, and surface roughness measurements were taken using a Zygo New View 7100 Profilometer with the Shrinky-Dink plastic surface set as the zero height reference plane.

The target geometry has a channel height of 65 μm and chevron height of 130 μm , both measured from the reference plane. Thus, two PDMS castings made from the template could be bound together to form a microfluidic device with 130 μm channel with 65 μm chevrons on each side. These measurements mean a channel : chevron aspect ratio of two, which is important to conserve in the prototype to match the microfluidic characteristics of the target geometry.

For the inkjet templates, the resulting height of the templates did not produce the desired height of our target geometry, but notably larger thicknesses were observed where chevrons were printed on top of the base geometry.

Adding additional layers had noticeable effects between printing two or four layers. As five or six layers were added, however, the thicknesses began to shrink drastically. This may be because beyond a certain height, the dried ink is stripped from the plastic as the printer arm slides by. It is also possible that weaker bonds form at the ink–ink interface compared to the ink–thermoplastic interface, causing fragments to break off during transport and testing. Regardless, a maximum value of 63 μm was achieved with this printing method. Sandwiching two PDMS halves together would then yield 100 μm channels with 10 μm chevrons at best.

Theoretically, these molds could be used as templates for casting microfluidic devices with PDMS. However, the rough surface of the thermoplastic sheet after baking causes the surface layer of the PDMS to be opaque rather than transparent, making chevron alignment impossible when binding two halves together. The surface roughness also makes it difficult to bind the two halves together by standard means of plasma

cleaning. They require a strong adhesive, causing further imperfections to the resultant microchannel. Although the geometries of these channels were in many regards a success, no valid use is able to come from the multilayer inkjet channels because of their inability to align and bind.

The laserjet templates yielded more desirable results than the inkjet. The lack of roughness and transparency was far greater than the inkjet counterparts. To understand the channel height resolution and roughness, laserjet templates were prepared and measured for one through four print layers/feature. The results of these findings are shown in Fig. 2. A single layer of ink produces channels approximately 32 μm thick. Surprisingly, additional ink layers don't have a linear correlation with feature height or roughness. However, the variance of the heights is quite low, so templates with uniform features can be made with predictable heights.

Profilometry showed a lack of spatial accuracy of the chevrons in both inkjet and laserjet templates. The highest points of the chevron geometry tended to lie where the gaps between the chevrons should have been located. It was hypothesized that the chevrons were actually overlapping each other after shrinking, and that better spatial accuracy could be obtained by spacing the chevrons 200 μm apart. This concept was combined with the hypothesis that less printing layers would eliminate spatial error, so only two layers per feature were selected for the 200 μm spacing template. The hypothesis was correct, and the surface profiles of the two different chevron templates are shown in Fig. 3.

To prove the functionality of the multilayer laserjet template, microfluidic devices were cast from the templates as described in the ESI.† From these devices, polymer fibers were produced according to literature,¹⁶ and the process is shown in Fig. 4. A solution of 2% polycaprolactone (PCL) polymer in 2,2,2-trifluoroethanol (TFE) was used as the core flow and 5% polyethylene glycol (PEG) in a 1 : 1 ratio of water and ethanol was used as the sheath flow. The core and sheath fluids were loaded into separate syringes and connected to the inlets of the microchannel. An automatic syringe pump was used to control the flow rates of the sheath and core flows. SEM images of the resulting fibers are shown in Fig. 5 along with their sheath and core fluid flow rates.

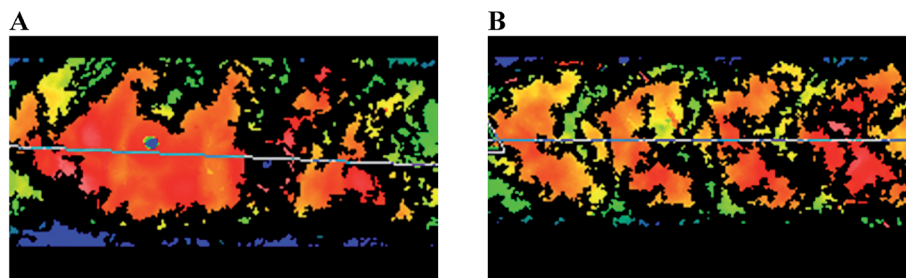


Fig. 3 (A) Surface profile of the 150 μm spaced chevrons and (B) 200 μm spaced chevrons. The 150 μm chevrons overlapped in printing, distorting them. The 200 μm spaced chevrons are highly accurate to their target geometry because they have few printing layers and no overlapping effect. Blue points represent heights close to the surface of the Shrinky-Dink plastic, red points represent heights that are extruded away from the surface, and black points represent areas where data was not acquired due to the area having a steeper slope than the equipment could process or it was out of the range of the profilometry scan.

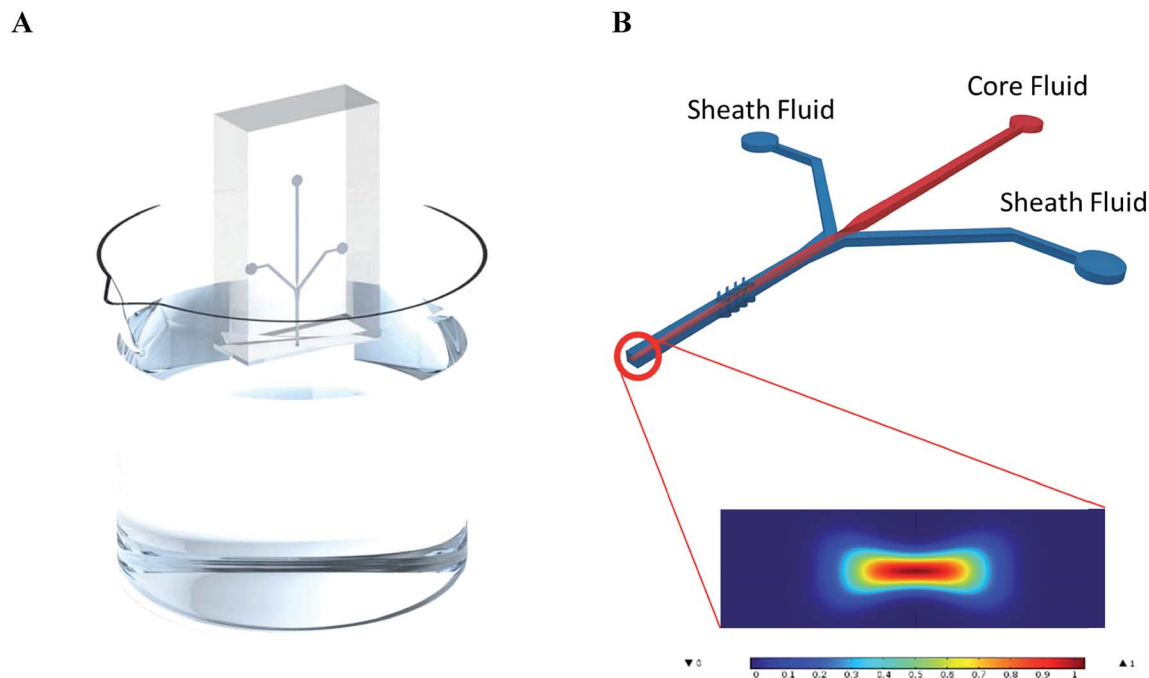


Fig. 4 Process for PCL microfiber creation. (A) A microfluidic channel is developed from the template and is submerged vertically into a beaker of water. PTFE tubes are inserted into the inlets of the device. (B) Schematic of the core and sheath flow trajectories. A COMSOL simulated result of the outlet with sheath and core flow rates set to $30 \mu\text{L min}^{-1}$ and $5 \mu\text{L min}^{-1}$ is shown. The color scale represents the concentration distribution, with 1 (red) representing pure core fluid and 0 (blue) representing pure sheath fluid. The colors between represent various degrees of mixing.

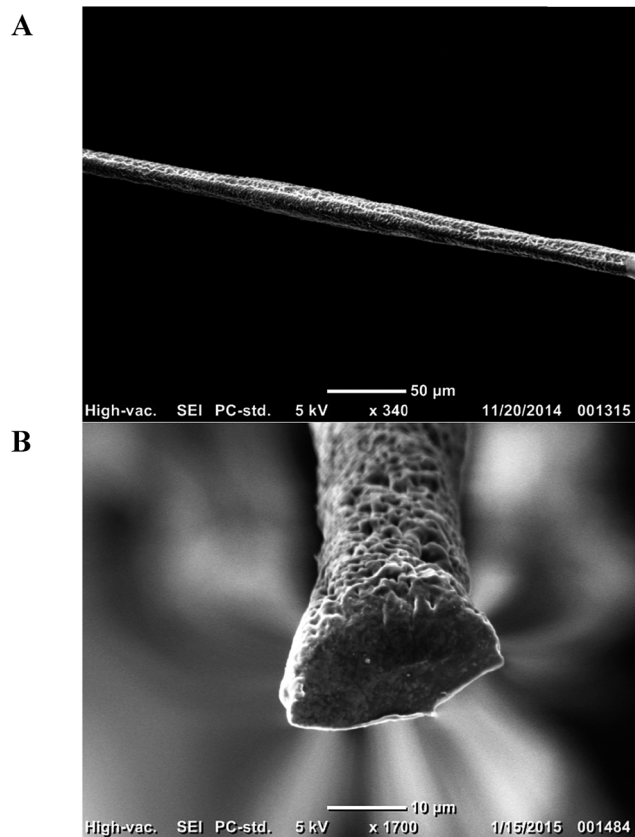


Fig. 5 SEM images of PCL microfibers. (A) Sheath and core flow rates set to $30 \mu\text{L min}^{-1}$ and $5 \mu\text{L min}^{-1}$. Thickness is approximately $17 \mu\text{m}$. (B) Cross section of a fiber with $30 \mu\text{L min}^{-1}$ and $5 \mu\text{L min}^{-1}$ flow rates.

Syringe pumps push core and sheath fluids through their respective inlets. The fluids meet at the intersection where the sheath flow concentrates the core fluid stream away from the sides of the channel. Simultaneously, the chevron grooves generate hydrodynamic lift which compresses the flow from the vertical walls.¹⁸ These two actions focus the core fluid to a narrow area at the center of the channel's cross section. The core fluid dries as it travels through the device due to contact with the sheath flow, which absorbs the TFE in the solution. With a long channel length, the core fluid reduces to a polymer microfiber.

This is a proof of concept that the thermoplastic templates can be used as a cheap method for rapid prototyping. The channels are capable of creating microfibers with control over the cross section and size by adjusting the core-sheath flow rate. $30/5 \mu\text{L min}^{-1}$ sheath/core flow resulted in fibers with a cross section of approximately $17 \mu\text{m}$. The COMSOL simulation in Fig. 4B closely matches the experimental results. Assuming the fiber is produced at 0.95 concentration and above (dark red) then the predicted diameter of the fiber fabricated under the $30/5 \mu\text{L min}^{-1}$ sheath/core flow scenario is $21.8 \mu\text{m}$. The physical shape of the COMSOL predicted result matches what we obtained experimentally at 78% the size. Microfibers have many uses, especially in the healthcare field. These microfibers do not require the same smoothness that is typical for optical fibers, and it has been suggested that fibers with porous morphologies make better scaffolds for cell growth.²⁰ This method has demonstrated its ability for making microfibers for healthcare applications faster and at a much lower cost than the other methods.

Table 1 Economic analysis of various microfluidic template generating methods

Method	Overhead materials required	Overhead cost	Materials required per template	Cost per template
Silicon wafer	Electric furnace, multi wire saw, UV light, polishing machine	\$500 000+	Blank silicon wafer, photoresist, mask, etchant	\$24
3D printing	3D printer	\$4000	Plastic	\$1.50
PMMA micromilling	Micromill, toolbits	\$6000–\$18 000	PMMA	\$0.50
Copper substrate	Laser printer	\$1600	Copper, dicing tape, various chemicals, special registration black toner	\$4.60
This work	Laser printer, conventional oven	\$1700	Shrinky-Dink shrinkable plastic, toner	\$0.40

An economic analysis of the different microfluidic template fabrication methods was conducted to better communicate the cost differences between them. Materials that are needed as a one-time overhead purchase as well as materials needed per fabricated microfluidic template were investigated. This information is shown in Table 1. It is important to note that estimated cost values were used in some cases where the information could not be found. A detailed explanation of how each cost value was acquired can be found in the ESI.†

Conclusions

The operations of microfluidic devices require highly accurate details with acute features. This prototyping method is limited in comparison to the high dimensional accuracy of silicon wafers, but many insights and uses are available with this method at a low cost. Feature heights can be controlled to heights over 100 μm by controlling the number of printing layers, and second layer features can be created with high spatial accuracy with a minimum separation distance of 200 μm . This leaves plenty of room for creating microfluidic designs for multiple functions, though it does require intelligent design from the researchers to control the aspect ratios. Primarily, this method can be used for fabricating microfibers for drug delivery in healthcare as demonstrated here. However, many microfluidic functions can be achieved with this method.

The method presented in this paper has plenty of room for improvement. There are many factors that influence the surface structure of the microfluidic templates that need to be considered in the design stages, such as the resolution of the printer, ink type, and print settings. Future research should be conducted that further investigates the relationship between these parameters and the quality of the template. Minimizing the amount of trips through the printer will increase the repeatability of manufactured templates. Printable materials other than powder and liquid ink could decrease the this number as well as increase the quality of the template surfaces, resulting in higher yields of templates that create functional microchannels without leakage or other undesirable qualities.

It is unlikely that optimization of this technique would be able to replace the highly accurate silicon wafer for situations where

ultra-high quality is needed. However, in situations where new microfluidic designs are needed in an on-going basis or at a low cost, the method proposed here becomes the favorable option. The cost to create each template is less than \$1 USD and can be made without expensive laboratory equipment or a clean-room facility.

Microfluidic molds were created with multilayer printing onto Shrinky-Dink thermoplastic sheets which were then shrunk and used as templates for creating PDMS microfluidic channels. Different printing methods and layer numbers were investigated, measured, and compared. Laserjet printing in general yields templates with better geometric accuracy and usability. Microchannels that were closest to the target geometry were used to create PCL microfibers to demonstrate the ability to rapidly prototype functional microfluidic templates with this method.

Acknowledgements

We would like to thank Kelly Christensen for help with designing schematic image. This work was funded in part by the Iowa State University Foundation, and in part by the U.S. Department of Energy Office of Science, Office of Workforce Development for Teachers and Scientists (WDTS) under the Science Undergraduate Laboratory Internship (SULI) Program at Ames Laboratory. We also acknowledge the Iowa State University Presidential Initiative for Interdisciplinary Research and Health Research Initiative (ISU-HRI) for partial support of this work.

References

- 1 L. Marle and G. M. Greenway, Microfluidic devices for environmental monitoring, *TrAC, Trends Anal. Chem.*, 2005, **24**, 795–802.
- 2 P. Asrar, M. Scur and N. Hashemi, Multi-Pixel Photon Counters for Optofluidic Characterization of Particles and Microalgae, *Biosensors*, 2015, **5**, 308–318.
- 3 N. Hashemi, J. S. Erickson, J. P. Golden and F. S. Ligler, Optofluidic characterization of marine algae using a microflow cytometer, *Biomicrofluidics*, 2011, **5**, 032009.
- 4 A. Dector, R. Escalona-Villalpando, D. Dector, V. Vallejo-Becerra, A. Chávez-Ramírez and L. Arriaga, *et al.*,

- Perspective use of direct human blood as an energy source in air-breathing hybrid microfluidic fuel cells, *J. Power Sources*, 2015, **288**, 70–75.
- 5 J. D. Caplin, N. G. Granados, M. R. James, R. Montazami and N. Hashemi, Microfluidic Organ-on-a-Chip Technology for Advancement of Drug Development and Toxicology, *Adv. Healthcare Mater.*, 2015, **4**, 1426–1450.
 - 6 E. R. Choban, L. J. Markoski, A. Wieckowski and P. J. Kenis, Microfluidic fuel cell based on laminar flow, *J. Power Sources*, 2004, **128**, 54–60.
 - 7 P. Agnihotri and V. Lad. *Membrane-less Fuel Cells: Microfluidic Fuel Cells*, 2015.
 - 8 J. Yang, S. Ghobadian, P. J. Goodrich, R. Montazami and N. Hashemi, Miniaturized biological and electrochemical fuel cells: challenges and applications, *Phys. Chem. Chem. Phys.*, 2013, **15**, 14147–14161.
 - 9 W. K. Tomazelli Coltro, C. M. Cheng, E. Carrilho and D. P. Jesus, Recent advances in low-cost microfluidic platforms for diagnostic applications, *Electrophoresis*, 2014, **35**, 2309–2324.
 - 10 H.-O. Song, J.-H. Kim, H.-S. Ryu, D.-H. Lee, S.-J. Kim and D.-J. Kim, *et al.*, *Polymeric LabChip real-time PCR as a point-of-care-potential diagnostic tool for rapid detection of influenza A/H1N1 virus in human clinical specimens*, 2012.
 - 11 J.-H. Wang, L. Cheng, C.-H. Wang, W.-S. Ling, S.-W. Wang and G.-B. Lee, An integrated chip capable of performing sample pretreatment and nucleic acid amplification for HIV-1 detection, *Biosens. Bioelectron.*, 2013, **41**, 484–491.
 - 12 Q. Zhu and D. Trau, Multiplex detection platform for tumor markers and glucose in serum based on a microfluidic microparticle array, *Anal. Chim. Acta*, 2012, **751**, 146–154.
 - 13 K. Kwapiszewska, A. Michalczyk, M. Rybka, R. Kwapiszewski and Z. Brzózka, A microfluidic-based platform for tumour spheroid culture, monitoring and drug screening, *Lab Chip*, 2014, **14**, 2096–2104.
 - 14 N. J. Cira, J. Y. Ho, M. E. Dueck and D. B. Weibel, A self-loading microfluidic device for determining the minimum inhibitory concentration of antibiotics, *Lab Chip*, 2012, **12**, 1052–1059.
 - 15 D. Sechi, B. Greer, J. Johnson and N. Hashemi, Three-Dimensional Paper-Based Microfluidic Device for Assays of Protein and Glucose in Urine, *Anal. Chem.*, 2013, **85**, 10733–10737.
 - 16 Z. Bai, J. M. Mendoza Reyes, R. Montazami and N. Hashemi, On-chip development of hydrogel microfibers from round to square/ribbon shape, *J. Mater. Chem. A*, 2014, **2**, 4878–4884.
 - 17 Y.-F. Li, M. Rubert, H. Aslan, Y. Yu, K. A. Howard and M. Dong, *et al.*, Ultraporous interweaving electrospun microfibers from PCL–PEO binary blends and their inflammatory responses, *Nanoscale*, 2014, **6**, 3392–3402.
 - 18 A. L. Thangawng, P. B. Howell Jr, J. J. Richards, J. S. Erickson and F. S. Ligler, A simple sheath-flow microfluidic device for micro/nanomanufacturing: fabrication of hydrodynamically shaped polymer fibers, *Lab Chip*, 2009, **9**, 3126–3130.
 - 19 M. A. Daniele, D. A. Boyd, A. A. Adams and F. S. Ligler, Microfluidic Strategies for Design and Assembly of Microfibers and Nanofibers with Tissue Engineering and Regenerative Medicine Applications, *Adv. Healthcare Mater.*, 2015, **4**, 11–28.
 - 20 Y. Jun, E. Kang, S. Chae and S.-H. Lee, Microfluidic spinning of micro- and nano-scale fibers for tissue engineering, *Lab Chip*, 2014, **14**, 2145–2160.
 - 21 A. Tamayol, M. Akbari, N. Annabi, A. Paul, A. Khademhosseini and D. Juncker, Fiber-based tissue engineering: Progress, challenges, and opportunities, *Biotechnol. Adv.*, 2013, **31**, 669–687.
 - 22 M. A. Daniele, S. H. North, J. Naciri, P. B. Howell, S. H. Foulger and F. S. Ligler, *et al.*, Rapid and continuous hydrodynamically controlled fabrication of biohybrid microfibers, *Adv. Funct. Mater.*, 2013, **23**, 698–704.
 - 23 D. A. Boyd, A. A. Adams, M. A. Daniele and F. S. Ligler, Microfluidic Fabrication of Polymeric and Biohybrid Fibers with Predesigned Size and Shape, *J. Visualized Exp.*, 2014, **83**, e50958, DOI: 10.3791/50958.
 - 24 H. Acar, S. Çınar, M. Thunga, M. R. Kessler, N. Hashemi and R. Montazami, Study of Physically Transient Insulating Materials as a Potential Platform for Transient Electronics and Bioelectronics, *Adv. Funct. Mater.*, 2014, **24**, 4135–4143.
 - 25 K. E. Petersen, Silicon as a mechanical material, *Proc. IEEE*, 1982, **70**, 420–457.
 - 26 F. Qian, Z. He, M. P. Thelen and Y. Li, A microfluidic microbial fuel cell fabricated by soft lithography, *Bioresour. Technol.*, 2011, **102**, 5836–5840.
 - 27 K. E. Herold and A. Rasooly. *Lab on a Chip Technology: Fabrication and microfluidics*, Horizon Scientific Press, 2009.
 - 28 D. Nguyen, D. Taylor, K. Qian, N. Norouzi, J. Rasmussen and S. Botzet, *et al.*, Better shrinkage than Shrinky-Dinks, *Lab Chip*, 2010, **10**, 1623–1626.
 - 29 A. D. Stroock and G. M. Whitesides, Components for integrated poly(dimethylsiloxane) microfluidic systems, *Electrophoresis*, 2002, **23**, 3461–3473.
 - 30 A. Grimes, D. N. Breslauer, M. Long, J. Pegan, L. P. Lee and M. Khine, Shrinky-Dink microfluidics: rapid generation of deep and rounded patterns, *Lab Chip*, 2008, **8**, 170–172.
 - 31 C.-S. Chen, D. N. Breslauer, J. I. Luna, A. Grimes, W.-c. Chin and L. P. Lee, *et al.*, Shrinky-Dink microfluidics: 3D polystyrene chips, *Lab Chip*, 2008, **8**, 622–624.
 - 32 M. Abdelgawad, M. W. Watson, E. W. Young, J. M. Mudrik, M. D. Ungrin and A. R. Wheeler, Soft lithography: masters on demand, *Lab Chip*, 2008, **8**, 1379–1385.
 - 33 G. Comina, A. Suska and D. Filippini, PDMS lab-on-a-chip fabrication using 3D printed templates, *Lab Chip*, 2013, **14**, 424–430.
 - 34 J. O'Connor, J. Punch, N. Jeffers and J. Stafford, A dimensional comparison between embedded 3D-printed and silicon microchannels, *J. Phys.: Conf. Ser.*, 2014, 012009.
 - 35 M. Grad, E. F. Young, L. Smilenov, D. J. Brenner and D. Attinger, A simple add-on microfluidic appliance for accurately sorting small populations of cells with high fidelity, *J. Micromech. Microeng.*, 2013, **23**, 117003.
 - 36 N. Hashemi, J. P. B. Howell, J. S. Erickson, J. P. Golden and F. S. Ligler, Dynamic reversibility of hydrodynamic focusing for recycling sheath fluid, *Lab Chip*, 2010, **10**, 1952–1959.